

DISTANCE-BASED CONTROL SYSTEM FOR MACHINE VISION-BASED SELECTIVE SPRAYING

B. L. Steward, L. F. Tian, L. Tang

ABSTRACT. For effective operation of a selective sprayer with real-time local weed sensing, herbicides must be delivered accurately to weed targets in the field. With a machine vision-based selective spraying system, acquiring sequential images and switching nozzles on and off at the correct locations are critical. An MS Windows-based imaging system was interfaced with a real-time embedded selective spray controller system to accomplish control tasks based on distance traveled. A machine vision-based sensing system and selective herbicide control system was developed and installed on a sprayer. A finite state machine (FSM) model was employed for controller design, and general design specifications were developed for determining the travel distance between states. The spatial application accuracy of the system was measured in the field using artificial targets. The system operated with an overall hit accuracy of 91% with no statistical evidence of hit accuracy or mean pattern length being dependent on vehicle speed. Significant differences in pattern length variance and mean pattern width were detected across speed levels ranging from 3.2 to 14 km/h. Spray patterns tended to shift relative to the target at higher travel speeds.

Keywords. Selective spray, Machine vision, Accuracy, Real-time, Control strategy.

Although most herbicide is applied uniformly in fields, the evidence is strong that weeds are not uniformly distributed, tending to grow in interspersed patches (Mortensen et al., 1995). The potential for reducing the quantity of herbicides applied, with accompanying economic and environmental benefits, has resulted in much research in the area of selective sprayers. For the effective operation of a selective sprayer, weed densities must be accurately sensed, and herbicide must be accurately applied where the weeds or weed patches are located, thereby achieving high spatial application accuracy (SAA).

Two approaches have been investigated for selective application of herbicides: those that apply herbicides relative to a map, and those that sense weeds in real-time with vehicle-mounted sensors. With map-based sprayers, the absolute positions of weed patches are stored prior to spraying in a GIS. Weed maps can be developed by several

means, including crop scouting (Stafford et al., 1996) and remote sensing (Brown et al., 1994; Lamb and Weedon, 1998; Bajwa and Tian, 2001). As the sprayer vehicle moves to a weed patch location, the application rate is adjusted to requirements for that weed patch. Spatial application error can come from several sources, including weed patch geo-referencing error in the original map (Bajwa and Tian, 2001), GPS error in sprayer position (Sullivan et al., 2001), and delays due to control system response (Rockwell and Ayers, 1994; Paice et al., 1995). Results from these studies show how the control systems can greatly impact SAA, and in turn spatial resolution, of selective spraying systems.

Another approach to variable-rate herbicide application is using sprayer-mounted sensors to sense weeds in real-time when herbicides are being applied. Such systems eliminate the need to determine absolute vehicle position within the field, thereby eliminating a major potential error source. Once a weed is sensed, however, the vehicle must travel the distance between the sensor and the nozzle before activating the nozzle. This distance must be measured accurately, and control must be precisely initiated to minimize spatial application error. In spite of the importance of both accurate sensing and precise control, much of the research thus far has focused on weed sensing and on the overall performance of the selective sprayer; relatively little has focused on the effect of the control system on SAA.

Sensor-based sprayers selectively turn on and off valves in the presence and absence of weeds, respectively. One typical sensing approach uses photodetectors to sense weeds. Hagger et al. (1983) reported on the development of a selective hand sprayer that used a pair of red and near-infrared (NIR) reflectance sensors for vegetation detection. In evaluations of this sprayer, over 90% of grass patch areas were killed in spite of delays in activating the nozzle. The analog circuit controlling this sprayer had no means for setting specific delays, as would be necessary for a vehicle

Article was submitted for review in October 2001; approved for publication by the Power & Machinery Division of ASAE in June 2002.

Journal Paper J-19809 of the Iowa Agriculture and Home Economics Experiment Station, Ames, Iowa, Project No. 4003, and supported by Hatch Act and State of Iowa funds. The use of trade names is only meant to provide specific information to the reader and does not constitute endorsement by Iowa State University or the University of Illinois.

The authors are **Brian L. Steward, ASAE Member Engineer**, Assistant Professor, Department of Agricultural and Biosystems Engineering, Iowa State University, Ames, Iowa; **Lei F. Tian, ASAE Member Engineer**, Associate Professor, Department of Agricultural Engineering, University of Illinois, Urbana, Illinois; and **Lie Tang, ASAE Member Engineer**, Assistant Professor, Department of Agricultural Sciences, The Royal Veterinary and Agricultural University, Taastrup, Denmark. **Corresponding author:** Brian L. Steward; Department of Agricultural and Biosystems Engineering, 206 Davidson Hall, Iowa State University, Ames, IA 50011; phone: 515-294-1452; fax: 515-294-2255; e-mail bsteward@iastate.edu.

selective sprayer. Shearer and Jones (1991) developed a selective sprayer that used NIR photodetector sensing of inter-row weeds. Time-delay relays were used to actuate nozzles after sensing weeds, but at only one speed. Whole-system evaluation of this sprayer revealed a 15% reduction in herbicide quantities with no statistical evidence of differences in weed control between selective and broadcast spraying. Merritt et al. (1994) developed a red and NIR photodetector pair weed detection system. This system was synchronized with pulses from a speed sensor. Evaluation of Detectspray, which employed a similar sensing system as Merritt et al., showed limitations at oblique sunlight angles and in detecting small weeds (Blackshaw et al., 1998). Patchen Weedseeker (Patchen, Inc., Ukiah, Cal.) used a speed sensor to determine when the nozzle should be turned on relative to a sensed weed (Beck and Vyse, 1995). The method used by the Weedseeker to control nozzle actuation has been not been described in the literature (Beck, 1996; Hanks and Beck, 1998). Reported evaluation of these systems has tended to focus on the overall efficacy of the systems instead of specific evaluation of how the control systems affect SAA.

Another approach to sensor-based selective spraying uses machine vision. Machine vision sensors can provide much higher spatial resolution data than photodetectors, thereby enabling the use of image processing for detecting weeds. Plant shape, texture, and color (Guyer et al., 1986; Franz et al., 1991; Burks et al., 2000; Zhang and Chaisattapagon, 1995) have all been investigated as possible image features for distinguishing weeds from crop plants. Another key difference between photodetector and machine vision weed sensing is that image processing often requires variable computation times for weed classification, a task which must be completed before nozzles arrive at weed patch locations. These real-time requirements complicate control system design.

Fan et al. (1998) developed a PC-based color machine vision system to acquire images of weeds and soybeans in a soil bin. By measuring the travel distance of the sensing carriage, sequential images were grabbed and processed with a maximum weed misclassification rate of 1.8%. This system was not interfaced with a spraying system, and thus was not evaluated for SAA. Lee et al. (1999) developed a machine vision weed sensing and selective herbicide control system for tomatoes. This system was used on a slow-moving vehicle (1.20 km/h) and had a small (11.43 cm × 10.16 cm) field of view (FOV) containing a tomato seedling row. The system was designed for a fixed vehicle speed with each nozzle activated for a fixed 10 ms time period after weed detection. Slaughter et al. (1999) developed an offset spray system that used machine vision sensing for selective weed control in roadside embankments. SAA of this system was not specifically measured. However, in overall system evaluation with artificial targets, overall target deposition was 57% with a 97% reduction in chemical applied, compared with a conventional sprayer.

Several different approaches can be used for selective sprayer control. Variable-rate control has been accomplished through closed-loop control around a chemical injection pump (Paice et al., 1995) or pulse-width modulation (PWM) flow control (Giles and Comino, 1990; Gopala Pillai et al., 1999). The major drawback with an injection system is the transport delay from the point of injection to the nozzles

(Paice et al., 1995). PWM flow control has the potential to offer a fast response, but in prototype closed-loop control systems, the response times have been slow unless feed-forward control was employed (Stone et al., 1999; Humburg et al., 2001). On/off control is another approach to selective spraying in which it is critical that the nozzles are activated when they are in close proximity to weed locations. One method to implement on/off control is to place the sensing results in a queue, thereby providing a delay based on (1) distance between sensors and nozzles and (2) vehicle speed (Merritt et al., 1994).

Another approach, and the one used in this article, is to model the selective spraying process as a finite state machine (FSM). FSMs are implementations of sequential logic that can only assume a set number of states. FSMs are widely used for control and decision-making logic in digital systems where outputs of systems are dependent on inputs and current states (Katz, 1994). An FSM is a good representation of a selective sprayer control system in which the system events (i.e., image acquisition and nozzle actuation) depend on distance traveled and current FSM state.

For machine vision-based selective spraying systems, little has been reported on the design and evaluation of the associated control systems, while minimizing sensing errors. This research specifically addresses these issues. The overall research objective was to develop a control system for a machine vision-based selective sprayer designed specifically for major Midwestern U.S. row crops (Steward and Tian, 1998, 1999). This system was specifically designed to accommodate a large FOV and to operate across a range of velocities up to 16 km/h. Specific research objectives were to:

- Develop a method for specifying where the controller FSM should shift from state to state.
- Measure control system accuracy in depositing spray relative to targets across three vehicle speed levels while minimizing the effect of sensing errors.

METHODS

A machine vision-based selective spraying system was designed and installed on a commercial sprayer. The control system was modeled as an FSM, and general design specifications were developed and implemented. Experimental methods were developed using artificial targets to minimize sensing errors and thus to better evaluate errors attributable to the control system.

EQUIPMENT

A Patriot XL (Tyler Industries Inc., Benson, Minn.) sprayer was retrofitted with a sensor boom and a Pulnix TMC-7EX (Sunnyvale, Cal.) color video camera was placed 3.35 m (11 ft) above and perpendicular to the ground surface and 3.09 m in front of the spray boom. A 6 mm Fujinon (Wayne, N.J.) auto-iris ($f/1.2$ to $f/360$) lens was used to focus on a 2.64 m × 3.48 m (104 in. × 137 in.) FOV with the shorter dimension in the direction of vehicle travel.

The composite video output of the camera was routed to a PXC200 PCI color frame grabber board (Imagenation Corp, Beaverton, Ore.), which was installed in a MegaPac (Dolch, Fremont, Cal.) portable computer with a 150 MHz Pentium

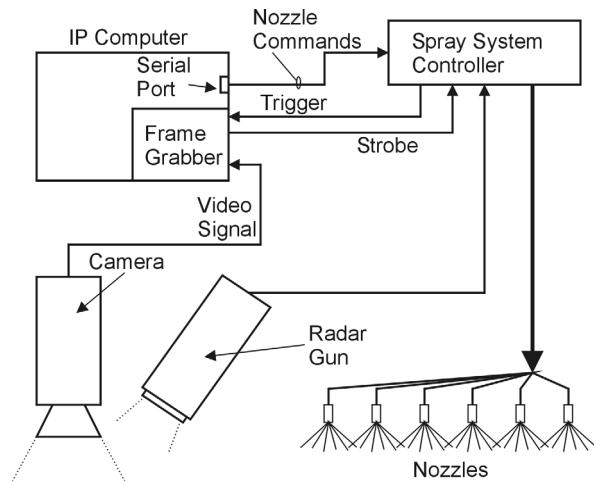


Figure 1. Block diagram showing the interconnection of components comprising the distance-based selective sprayer control system.

CPU. The frame grabber had a resolution of 640×486 pixels and converted the analog video signal to 24-bit digital color images. Because of interactions between interlacing and camera motion, video fields were captured, effectively halving the vertical resolution. This image processing (IP) computer acquired and segmented images, determined the location of target objects relative to fixed control zones in images, and sent control codes over a 9600 baud RS-232 serial link to a spray system controller (fig. 1).

The spray system controller was built around a TinyDrive (Tern, Davis, Cal.) single-board computer with an 8 MHz microcontroller. This controller received the commands from the IP computer and a square-wave pulse train proportional to vehicle ground speed. Synchro (Capstan Ag Systems, Topeka, Kansas) solenoid valves were mounted on check valve ports of standard nozzle bodies. The spray system controller directed a 12 VDC signal to the solenoid valves through solid-state relays to activate valves. A radar ground speed sensor (Dickey-John, Auburn, Ill.) was used to measure the distance traveled. This device was calibrated according to a standard commercial procedure (Raven Ind., Sioux Falls, S.D.) and produced 97.7 pulses/m.

DISTANCE-BASED SPRAY SYSTEM CONTROLLER DESIGN

The spray system controller synchronized control system events, such as image acquisition and nozzle actuation, according to an FSM model based on sprayer travel distance. The IP computer used Windows 95 (Microsoft, Redmond, Wash.), a co-operative multitasking operating system, and thus the image processing time was variable. Since the IP computer was triggered by the controller to acquire images, variations in image processing time did not affect system performance as long as results were available before they were needed by the spray system controller.

The FOV was divided into regions called control zones, and nozzles were activated based on detections in individual control zones. Control zones were 0.61 m (2 ft) long in the travel direction and 0.51 m (20 in.) wide, corresponding to the spray pattern of the nozzle directly behind them (fig. 2). The usable image area was a 4×6 matrix of control zones measuring 2.44 m high by 3.05 m wide that consisted of the number of complete control zones that fit in the FOV.

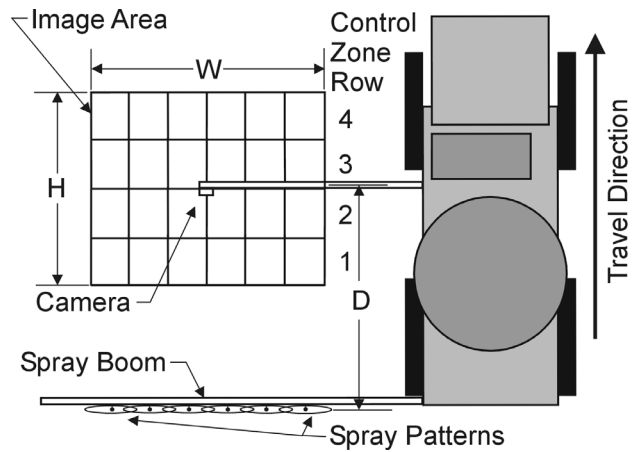


Figure 2. Physical configuration of the image area and spray nozzles. The image is divided into six columns and four rows of control zones, resulting in a 2.44 m high \times 3.05 m width usable image area. The camera was mounted 3.09 m ahead of the spray boom.

The spray system controller was connected to the IP computer by three links. First, a trigger line was used by the spray system controller to command the IP computer to acquire an image. Second, a strobe line was used to indicate to the spray system controller that an image had been acquired. Third, a RS-232 serial communication line was used to send individual nozzle commands after processing each control zone row.

Spray System Controller Software

The spray system controller software was modeled as an FSM with inputs of distance traveled, strobe signal, and elapsed time (fig. 3). When power was applied to the spray system controller, it entered an initialization state in which the controller issued triggers to the IP computer until a strobe was received back. Then, the controller was in a loop of states in which it initiated control for each control zone row and triggered the IP computer after appropriate travel distances, determined using the general design methodology described below. Since distance was measured from two image acquisitions locations, two distance counters were needed: an image acquisition counter and a control counter.

Other functions were done asynchronously from the FSM loop of the program as those data became available. Distance was counted by both counters using an interrupt service routine activated on every falling edge of the radar sensor pulse train. Another interrupt routine serviced the strobe signal. Control codes were received at the serial port and were stored in a circular buffer until they were needed at new control zone rows.

Image Processing System

The image processing software generated a graphical user interface that displayed image processing results and facilitated software setting changes. Through an interactive calibration window, a region in HSI color space that corresponded to the object color was specified for image segmentation. A look-up table (LUT) was then created in computer memory. Segmentation was accomplished by using the red, green, and blue intensities of each pixel to index the LUT. The classification for each pixel was then returned from the LUT (Tian and Slaughter, 1998).

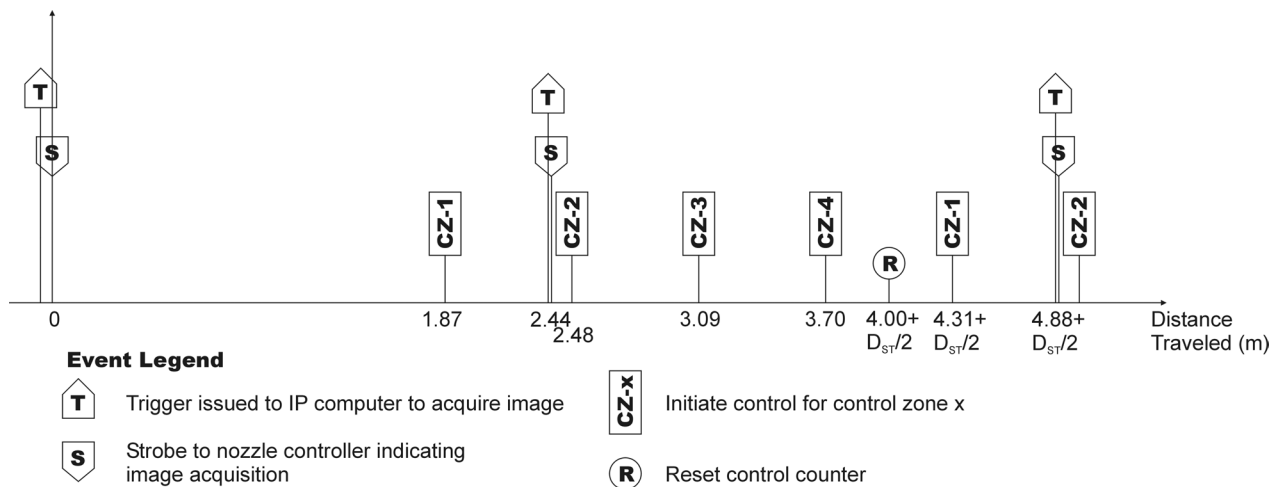


Figure 4. System events based on distance from initial image and physical configuration of the system used in the research. D_{ST} is the distance traveled between the trigger and strobe signals.

image, $N - 1$ control zone lengths, and one half of the last control zone length. This distance (d_{ca}) can thus be written as:

$$d_{ca} = D + \frac{H}{2} - \frac{H}{2N} \quad (6)$$

Using these general specifications for the specific configuration used in this research, the travel distances for FSM transitions were calculated (fig. 4). In addition, the processing time constraints required at a maximum speed of 16 km/h were $T_{FZ} < 0.418$ s and $\bar{T} < 0.136$ s.

EXPERIMENTAL PROCEDURE

A reduced system consisting of the IP computer and the spray system controller was tested in the lab with a function generator simulating a speed input from a speed sensor. The time between the trigger and the strobe signals was measured as the speed input frequency was varied to determine the speed at which the processing time constraints were limiting. The elapsed time for the image processing was also measured.

A controller test-mode experiment was performed in the field. Opaque white plastic sheeting, 152 μm (6 mil) thick, was placed over a 2.44 m \times 12.2 m (8 ft \times 40 ft) test area. The plastic was used so that a visible and measurable spray deposition pattern would result when dyed water was sprayed. A mixture of 378 L (100 gal) water to approximately 355 mL (12 oz) of pink dye (Precision Laboratories, Inc, Northbrook, Ill.) was placed in the sprayer tank. The original fluid delivery system of the Patriot sprayer was used with modifications to a 3.05 m (10 ft) boom section. Synchro solenoid valves were mounted to nozzle bodies in this section. Hose drops 0.381 m (15 in.) long were connected to the nozzle bodies so that the TeeJet 8006VS nozzles (Spraying Systems Co., Wheaton, Ill.) were 0.36 to 0.38 m (14 to 15 in.) above the surface being sprayed to achieve a control zone width of 0.51 meters. The boom pressure was set at 172 kPa (25 psi) to achieve a flow rate of 1.8 L/min (0.47 gal/min) per nozzle, which resulted in a spray deposition pattern that was visible over the range of travel velocities. The IP computer program was first put in the test

mode, which turned on alternate sets of three adjacent nozzles for every zone row, and the plastic covered area was sprayed at three travel speed levels: 3.2 to 3.9 km/h (2.0 to 2.4 mph), 6.9 to 8.7 km/h (4.3 to 5.4 mph), and 11 to 14 km/h (7.0 to 8.5 mph). A randomized complete block experimental design was used. The experiment was blocked by replication to reduce the effect of time-varying environmental conditions on the analysis. Each block consisted of a sprayer pass at each speed level. For each speed level replication, 18 to 20 sample measurements were taken of individual pattern lengths. The SAS (SAS Institute, Cary, N.C.) General Linear Model procedure (GLM) was used to test for significant differences in length across speed levels.

A target experiment used ten 0.191 m (7.5 in.) square yellow-colored paper targets, which were placed randomly on the plastic-covered area. The targets were inserted into clear Ziploc plastic bags for protection from the water. The target area corresponded to 595 pixels in the image. Nozzles were activated if more than 100 target pixels were detected in individual control zones.

The spray pattern width and length at each target was measured. Distances from the centers of targets to the start of patterns and the end of patterns were also measured. If the spray pattern was found on the target, a “hit” was noted for that target. These measurements were taken with the sprayer traveling at the same three speed levels listed above. A randomized block design was used. The experiment was blocked by replication to reduce the effect of variation of environmental conditions with time on the analysis. Each of the five blocks consisted of a sprayer pass at each speed level with 10 targets. The GLM procedure was used to analyze the dimensional data with speed level as a fixed effect factor. For the pattern width model, the number of nozzles turned on for a target was a model factor. The pattern length, distances to pattern start, and pattern end models included a factor accounting for the number of sequential zones in which a nozzle was actuated for a target. For models where significance was detected, the Tukey test was used to compare least squared means across speed levels. The categorical hit or miss data were analyzed using the chi-squared test for independence between speed level and hit accuracy.

RESULTS AND DISCUSSION

LAB TEST RESULTS

The time between the issuance of the trigger and the strobe signals varied from 0.018 s to 0.033 s for simulated low ground speeds. When this time increased, it indicated that image processing of the previous image was not completed when the trigger was issued. As the simulated ground speed was increased, the time between trigger and strobe did not increase until 18 km/h (11 mph). The first control zone row processing time varied from 0.160 s to 0.220 s, as measured by the image processing software, while the average processing time for all control zones varied from 0.095 s to 0.110 s. These measured times were all less than the processing time constraints shown above.

TEST MODE FIELD TEST RESULTS

The spray pattern lengths produced in the test mode were approximately normally distributed with a mean of 0.605 m (1.98 ft) and a standard deviation of 0.0487 m (0.160 ft). There was no statistical evidence of mean length dependency on speed level ($P = 0.67$). The standard deviation, however, was significantly larger at the low speed level than at the middle and high speed levels based on the modified Levene test (Conover et al., 1981). This revealed that the system was measuring distance within the reported accuracy of the speed sensor and initiating the control according to the 0.610 m (2 ft) control zone specification (table 1).

TARGET FIELD TEST RESULTS

The overall hit accuracy of the system was 91% (table 2). The hit accuracy was 96% for the lowest speed level. The hit accuracy decreased with increasing speed, with 90% for the middle speed level, and 86% for the highest speed level. From the chi-squared test, however, there was no statistical evidence to reject the hypothesis that the hit accuracy of the system was independent of speed. Two types of errors were observed. For five targets, no spray pattern was observed anywhere in the vicinity of the target, suggesting that the target was not correctly segmented as a target by the IP computer and was thus an error due to sensing. For the

Table 1. Comparison of spray pattern length with controller in test mode.

Speed Level (km/h)	Mean Pattern Length (m)	Pattern Length Variance (m)
3.2 to 3.9	0.601a ^[a]	0.070a ^[b]
6.9 to 8.7	0.605a	0.037b
11 to 14	0.608a	0.031b

^[a] Letters indicate Duncan's multiple range test group within a column at the 0.01 significance level.

^[b] Letters indicate grouping by modified Levene test for constant variance at the 0.01 significance level.

Table 2. Contingency table of target hits and misses by speed level.

Speed Level (km/h)	Number of Targets Not Hit	Number of Targets Hit	Total Number of Targets	Accuracy (%)
3.2 to 3.9	2	48	50	96
6.9 to 8.7	5	45	50	90
11 to 14	7	43	50	86
Totals	14	136	150	91

remaining nine missed targets, there was a spray pattern near the target, but the spray did not hit the target.

The distribution of spray pattern length for the target experiments was bimodal, with one mode centered at approximately 0.60 m (24 in.) and the other around 1.2 m (48 in.) (fig. 5). The pattern widths data also followed a bimodal distribution, with one mode center at approximately 0.425 m (17 in.) and the other at 0.85 m (33 in.) (fig. 6). The bimodality was expected because when the target was on a control zone boundary, the IP computer would command the controller to spray in two adjacent control zones if the number of object pixels was above the threshold for both control zones. The spray pattern length or width would thus correspond to one or two adjacent control zones. Both multiple zone width and length factors were included in the appropriate statistical models to account for the variation due to this random effect. Least squared means were compared across speed levels with the Tukey test because of the unbalanced design in the multiple zone factors.

The GLM F-test identified significant differences in the spray pattern width ($F_{2,136} = 21.38$; $P < 0.0001$) across speed levels. The Tukey test identified significant differences between the least squared mean width at every speed level (table 3). This result revealed an interaction between the

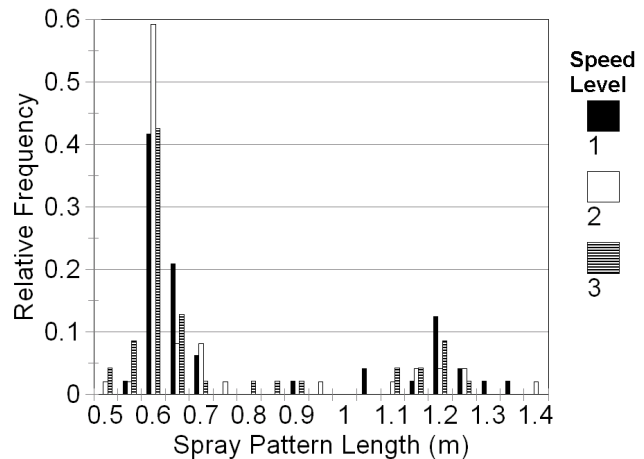


Figure 5. Histograms of the spray pattern length by speed level. Distributions are bimodal with no observable differences in means across speeds.

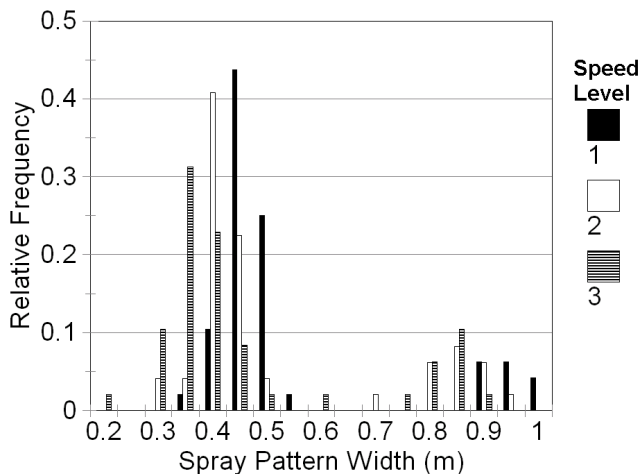


Figure 6. Histograms of the spray pattern width by speed level. Distributions are bimodal with decreases in mean width with increasing speed.

Table 3. Comparison of mean spray pattern dimensions and distances from target by speed level.

Number of Adjacent Patterns	Speed Level (km/h)	Pattern Width (m)	Pattern Length (m)	Distance to End of Pattern (m)	Distance from Start of Pattern (m)
1	3.2 to 3.9	0.48a ^[a]	0.64a	0.38a	0.26a
	6.9 to 8.7	0.43b	0.64a	0.53b	0.11b
	11 to 14	0.39c	0.64a	0.50b	0.15ab
2	3.2 to 3.9	0.97	1.2	0.71	0.50
	6.9 to 8.7	0.87	1.2	0.80	0.41
	11 to 14	0.83	1.2	0.78	0.47

^[a] Letters indicate groupings of least squared means based on Tukey test at the 0.01 significance level.

spray pattern and speed: the pattern width decreased as the speed increased. This pattern collapse should be taken into account in the design of selective sprayers since such sprayers will not be able to rely on pattern overlap for uniform coverage when individual nozzles are activated.

Tukey's test did not detect significant differences in least squared mean pattern lengths. This insensitivity to vehicle speed was consistent with the test mode results. The least squared mean distances between target center and pattern start and end had significant differences across speed levels. The distance to the end of the spray pattern tended to increase with speed, and the distance to the pattern start tended to decrease with speed. The distance from pattern start to target center was also less than that to the pattern end across all speed levels. These results revealed a shift of the spray pattern relative to the target in the direction of travel at all speeds and an increase in this shift at the higher speeds.

ERROR ANALYSIS

Several sources of error were identified that impacted the system SAA. First, the radar speed sensor had a reported accuracy of $\pm 1\%$ to $\pm 3\%$ after calibration, and decreasing accuracy at lower speeds (Dickey John, Auburn, Ill.). Sensor fusion of encoders and DGPS is being investigated as a more accurate distance and position sensing system (Zhou et al., 2000). Another source of error in the sensing system arose from the timing of the video signal. Since the video signal was not synchronized with the trigger, some distance passed until the start of a new image field when the frame grabber could start acquiring the field after a trigger. Because the spray system could measure the distance traveled between trigger and strobe, the error introduced could be partially corrected without any additional measurements. This resulted in an error ranging from 0 to 0.037 m (1.5 in.) at 16 km/h. Pitch and roll of the vehicle was another source of sensing error due to the shifting of the FOV of the camera. Based on the geometry of the camera on the sprayer, a 1° change in the pitch resulted in a FOV shift on the order of 0.025 m (1 in.). In addition, the camera lens caused radial image distortion. From a calibration image, the maximum error due to lens distortion was estimated to be about 0.025 m (1 in.). This distortion can be eliminated using camera calibration and distortion removal algorithms.

The observed shift in the spray pattern relative to the target was introduced by a lag in the control system. One primary source of error in the control system that led to this delay was the time required to pressurize the hose drops and the time for the spray to travel from the nozzle to the ground surface. The

delay between the excitation signal and the fluid exiting the nozzle was measured experimentally to be 0.012 s when turning on and a maximum of 0.034 s when turning off. At the maximum vehicle speed, this delay would result in a shift of 0.053 m (2.2 in.) in the start of the pattern and a shift of 0.15m (6 in.) in the pattern's end. It would be possible to adjust for this delay by adjusting the nozzle activation distance (d_{cz}) based on vehicle speed.

CONCLUSIONS

A control system was developed for a machine vision-based selective sprayer. This sprayer design accommodated a large FOV and was able to operate across a wide range of vehicle speeds. This study showed that:

- A finite state machine model is an effective tool in the design of a selective sprayer controller. The FSM model was useful for moving from a physical sprayer configuration to a controller software design. In addition, the FSM model found utility in determining time constraints and analyzing sources of error.
- By using an experimental design in which sensor classification error was minimized, the controller performance could be analyzed more specifically. In particular, no significant differences were detected in accuracy or mean pattern length across speed levels, but a spray pattern shift relative to the target was detected. Interaction between the spray pattern width and speed level was detected and must be taken into account in the design of selective sprayers.

ACKNOWLEDGEMENTS

Additional support for this research came from the Illinois Council of Food and Agricultural Research, Inc. (C-FAR) and the University of Illinois (Project Nos. 97I-124-3 and 99I-112-3 AE).

REFERENCES

- Bajwa, S. G., and L. F. Tian. 2001. Aerial CIR remote sensing for weed density mapping in a soybean field. *Trans. ASAE* 44(6): 1965-1974.
- Beck, J. 1996. Reduced herbicide usage in perennial crops, row crops, fallow land, and non-agricultural applications using optoelectronic detection. In *New Trends in Farm Machinery Development and Agriculture*, SP-1194: 11-17. Warrendale, Pa.: SAE.
- Beck, J., and T. Vyse. 1995. Structure and method usable for differentiating a plant from soil in a field. U.S. Patent No. 5389781.
- Blackshaw, R. E., L. J. Molnar, D. F. Chevalier, and C. W. Lindwall. 1998. Factors affecting the operation of the weed-sensing Detectspray system. *Weed Science* 46(1): 127-131.
- Brown, R. B., J.-P. G. A. Steckler, and G. W. Anderson. 1994. Remote sensing for identification of weeds in no-till corn. *Trans. ASAE* 37(1): 297-302.
- Burks, T. F., S. A. Shearer, R. S. Gates, and K. D. Donohue. 2000. Backpropagation neural network design and evaluation for classifying weed species using color image texture. *Trans. ASAE* 43(4): 1029-1037.
- Conover, W. J., M. E. Johnson, and M. M. Johnson. 1981. A comparative study of tests for homogeneity of variances, with applications to the outer continental shelf bidding data. *Technometrics* 23(4): 351-361.

- Fan, G., N. Zhang, D. E. Peterson, and T. M. Loughin. 1998. Real-time weed detection using machine vision. ASAE Paper No. 983032. St. Joseph, Mich.: ASAE.
- Franz, E., M. R. Gebhardt, and K. B. Unklesbay. 1991. Shape description of completely visible and partially occluded leaves for identifying plants in digital images. *Trans. ASAE* 34(2): 673–681.
- Giles, D. K., and J. A. Comino. 1990. Droplet size and spray pattern characteristics of an electronic flow controller for spray nozzles. *J. Agric. Eng. Research* 47(4): 249–267.
- Gopala Pillai, S., L. Tian, and J. Zheng. 1999. Evaluation of a flow control system for site-specific herbicide application. *Trans. ASAE* 42(4): 863–870.
- Guyer, D. E., G. E. Miles, M. M. Schreiber, O. R. Mitchell, and V. C. Vanderbuilt. 1986. Machine vision and image processing for plant identification. *Trans. ASAE* 29(6): 1500–1507.
- Haggar, R. J., C. J. Stent, and S. Isaac. 1983. A prototype hand-held patch sprayer for killing weeds, activated by spectral differences in crop/weed canopies. *J. Agric. Eng. Research* 28(4): 349–358.
- Hanks, J. E., and J. L. Beck. 1998. Sensor-controlled hooded sprayer for row crops. *Weed Technology* 12(2): 308–314.
- Humburg, D. S., B. L. Steward, and X. Chen. 2001. Control simulation and modeling of a PWM sprayer system in variable-rate chemical application. ASAE Paper No. 013034. St. Joseph, Mich.: ASAE.
- Katz, R. H. 1994. *Contemporary Logic Design*. Redwood City, Cal.: Benjamin/Cummings Publishing.
- Lamb, D. W., and M. Weedon. 1998. Evaluating the accuracy of mapping weeds in fallow fields using airborne digital imaging: *Panicum effusum* in oilseed rape stubble. *Weed Research* 38(6): 443–451.
- Lee, W. S., D. C. Slaughter, and D. K. Giles. 1999. Robotic weed control system for tomatoes. *Precision Agric.* 1(1): 95–113.
- Mortensen, D. A., G. A. Johnson, D. Y. Wyse, and A. R. Martin. 1995. Managing spatially variable weed populations. In *Site-Specific Management for Agricultural Systems*, 397–415. P. C. Roberts, R. H. Rust, and W. E. Larson, eds. Madison, Wisc.: ASA-CSSA-SSSA.
- Merritt, S. J., G. E. Meyer, K. Von Bargen, and D. A. Mortensen. 1994. Reflectance sensor and control system for spot spraying. ASAE Paper No. 941057. St. Joseph, Mich.: ASAE.
- Paice, M. E. R., P. C. H. Miller, and J. D. Bodle. 1995. An experimental sprayer for the spatially selective application of herbicides. *J. Agric. Eng. Research* 60(2): 107–116.
- Rockwell, A. D., and P. D. Ayers. 1994. Variable-rate sprayer development and evaluation. *Applied Eng. in Agric.* 10(3): 327–333.
- Shearer, S. A., and P. T. Jones. 1991. Selective application of post-emergence herbicides using photoelectrics. *Trans. ASAE* 34(4): 1661–1666.
- Slaughter, D. C., D. K. Giles, and C. Tauzer. 1999. Precision offset spray system for roadway shoulder weed control. *J. Transportation Eng.* 125(4): 364–371.
- Stafford, J. V., J. M. Le Bars, and B. Ambler. 1996. A hand-held data logger with integral GPS for producing weed maps by field walking. *Computers and Electronics in Agric.* 14(3): 2235–2247.
- Steward, B. L., and L. F. Tian. 1998. Real-time weed detection in outdoor field conditions. In *Proc. SPIE 3543: Precision Agriculture and Biological Quality*, 266–278. G. E. Meyer and J. A. DeShazer, eds. Bellingham, Wash.: SPIE.
- _____. 1999. Machine vision weed density estimation for real-time outdoor lighting conditions. *Trans. ASAE* 42(6): 1897–1909.
- Stone, M. L., D. K. Giles, and K. J. Dieball. 1999. Distributed network system for control of spray droplet size and application rate for precision chemical application. ASAE Paper No. 993112. St. Joseph, Mich.: ASAE.
- Sullivan, M., M. R. Ehsani, J. T. Walker, P. Levison, and L. Lang. 2001. Accuracy and availability of WAAS for precision agriculture. ASAE Paper No. 011155. St. Joseph, Mich.: ASAE.
- Tian, L. F., and D. C. Slaughter. 1998. Environmentally adaptive segmentation algorithm for outdoor image segmentation. *Computers and Electronics in Agric.* 21(3): 153–168.
- Zhou, Y., L. Tian, and L. Tang. 2000. Improving GPS positioning precision by using optical encoders. In *Proc. 3rd IEEE International Conference on Intelligent Transportation Systems*, 293–298. Piscataway, N.J.: IEEE.
- Zhang, N., and C. Chaisattapagon. 1995. Effective criteria for weed identification in wheat fields using machine vision. *Trans. ASAE* 38(3): 965–975.